Onset of frictional slip by domain nucleation in adsorbed monolayers

Marco Reguzzoni[a], Mauro Ferrario[a], Stefano Zapperi[a,b,1], and Maria Clelia Righi[a]

[a]Consiglio Nazionale delle Ricerche, Istituto Nazionale per la Fisica della Materia - S3 and Dipartimento di Fisica, Università di Modena e Reggio Emilia, Via G. Campi 213/A, I-41100, Modena, Italy; and [b]Istituto Nazionale per la Fisica della MateriaInstitute for Scientific Information Foundation Viale San Severo 65, 10133 Turin, Italy

It has been known for centuries that a body in contact with a substrate will start to slide when the lateral force exceeds the static friction force. Yet the microscopic mechanisms ruling the crossover from static to dynamic friction are still the object of active research. Here, we analyze the onset of slip of a xenon (Xe) monolayer sliding on a copper (Cu) substrate. We consider thermal-activated creep under a small external lateral force, and observe that slip proceeds by the nucleation and growth of domains in the commensurate interface between the film and the substrate. We measure the activation energy for the nucleation process considering its dependence on the external force, the substrate corrugation, and particle interactions in the film. To understand the results, we use the classical theory of nucleation and compute analytically the activation energy which turns out to be in excellent agreement with numerical results. We discuss the relevance of our results to understand experiments on the sliding of adsorbed monolayers.

commensurate interface | creep | depinning | friction | quartz crystal microbalance (QCM)

Understanding the microscopic mechanisms that govern friction represents a fundamental scientific problem with important practical applications. According to the macroscopic description dating back to Amontons and Coulomb, two bodies in contact under a normal force F_N start to slide when subject to a lateral force exceeding the static friction force $F_s = \mu_s F_N$, while sliding motion can be sustained under a dynamic friction force $F_d = \mu_d F_N$, where the friction coefficients typically obey $\mu_d \leq \mu_s$. The transition from static to dynamic friction is not completely well defined, because even when the lateral force is below the nominal static friction, a body can slowly creep forward due to thermal activation (1, 2). In addition, direct visualization of the contact area at the onset of slip (3) and numerical simulations (4) indicate the formation and propagation of detachment fronts fracturing the multicontact interface. These findings suggest that the onset of slip is due to microscopic processes, ultimately due to the interactions between individual atoms lying on the surfaces in contact, propagating up to the macroscale to yield collective sliding.

A convenient setup to investigate the microscopic origin of friction is provided by a one-atom thick film—a monolayer—adsorbed on a perfect crystalline surface. This idealized system has been studied numerically by molecular dynamics simulations (5–9) and experimentally by using a QCM (10–12). In the QCM, a noble gas monolayer is deposited on a resonating quartz crystal covered by a metallic substrate. The resonant oscillations of the crystal induce inertial forces on the monolayer causing it to slip with respect to the substrate. Whether this can happen depends on the crystal structure and the relative orientation of the surfaces in contact. When each atom in the monolayer falls into a minimum of the substrate potential, the interface is said to be commensurate and the forces induced by the QCM are usually too weak to displace it. Otherwise, the interface is incommensurate and sliding occurs even for extremely low lateral forces. Hence, one would be tempted to conclude that the ubiquitous

static friction should be associated with a commensurate interface (5), except that most surfaces in contact form incommensurate interfaces. It has been suggested that this paradox might be resolved by the presence of a fluid layer between the solid interfaces (13), or by the unavoidable surface roughness which implies that real contact occurs through a small set of interlocked asperities (14). In either case, relating atomistic slip mechanisms to macroscopic friction is still an open issue.

In this paper, we study the onset of slip in a monolayer of Xe atoms adsorbed on a Cu surface by molecular dynamics simulations based on a realistic potential for the film-substrate interaction (15). Here, we concentrate on the creep dynamics observed when the applied lateral force is smaller than the nominal ($T = 0$) static friction force F_s. In this case the film sets into motion only because of thermal activation. We compute the slip activation time as a function of temperature and find an Arrhenius law from which we estimate the associated energy barrier. This barrier turns out to be smaller than naively expected from the action of the substrate potential on individual Xe atoms and leads to a smaller effective static friction force. A direct visualization of the monolayer structure during slip reveals the nucleation of a commensurate domain that then expands, causing the sliding of the entire film. To understand quantitatively this phenomenon, we resort to the classical theory of nucleation and compute the associated energy barrier. This energy depends on the surface energy of the domain wall separating the two commensurate regions. Hence, we study the domain wall conformation and energy in the continuum limit and test the solution numerically for a simple configuration. Inserting this result in the nucleation theory, we obtain an excellent agreement for the nucleation barrier as a function of the film interparticle and substrate interactions.

Friction in the Xe/Cu interface was studied experimentally by using the QCM (11) revealing that the monolayer was slipping in spite of the commensurate structure of the interface (16). This result was attributed in ref. (11) to the relatively weak substrate force, but our analysis shows that the lateral force provided by the QCM is still many orders of magnitude smaller than this. The onset of slip in commensurate interfaces can be described as a nucleation process and is thus analogous to other first order phase transitions, such as the switching of ferromagnetic materials or the condensation of a liquid from a gas. This analogy suggests that defects may act as seeds for the new phase, lowering the nucleation barrier. This is confirmed by numerical simulations introducing a small density of vacancies in the Xe film. In this case, we witness a decrease by several orders of magnitude of the nucleation time so that the film slips even under a very low

lateral force. This is due to the presence of extended domain walls that are pinned only by a very weak potential (17), suggesting an explanation for the low static friction observed experimentally in ref. (11).

Model

The Substrate Potential. The interaction of a rare gas atom with a metal surface of van der Waals nature is attractive at long distances and highly repulsive at short distances where the metal charge distribution overlaps with the rare gas closed shells (18). In our simulations, we describe the potential energy surface for a Xe atom on the Cu(111) surface by means of a three-dimensional function derived by fitting the results of ab initio calculations (15):

$$V(x,y,z) = A_0(x,y)\exp(-z/A_1(x,y)) - A_2(x,y)/z^3.$$

The potential is the sum of a repulsive term presenting a z-dependence that mimics the exponential decay of the surface charge density into the vacuum and of an attractive term proportional to z^{-3} as the polarization potential (18). The in-plane variation of V is governed by the parameters A_i which are 2D functions presenting the same periodicity of the surface and can thus be expanded in the Bloch form: $A_i(x,y) = A_i^{top} + \Delta_i u(x,y)$, with $u(x,y) = [3 - \sum_{\mathbf{g}} \cos(\mathbf{g} \cdot \mathbf{r})]$. The sum runs over the first three reciprocal vectors $\mathbf{g}$ of the triangular lattice:

$$\sum_{\mathbf{g}} \cos(\mathbf{g} \cdot \mathbf{r}) = 2\cos\theta_x\cos\theta_y + \cos 2\theta_y,$$

$$\theta_x = \frac{2\pi x}{a}; \qquad \theta_y = \frac{2\pi y}{a\sqrt{3}} \qquad \qquad [1]$$

The prefactor $\Delta_i = (A_i^{ho} - A_i^{top})/\delta$ measures the difference between the value of A_i at top and hollow sites. We introduce a tunable factor δ in order to quantitatively reproduce the value of the potential corrugation obtained experimentally from phonon dispersion curves measured by inelastic scattering of He atoms (19). In particular, we tune δ so that the value of the corrugation along the sliding direction, corresponding to the minimum energy path between two equivalent potential minima, is $V_0 = 1.9$ meV as reported in ref. (19). The functional form of the parameter A_0 is related to that of the parameter A_1 according to the following expression:

$$A_0(x,y) = A_0^{top}\exp\left(\frac{\alpha(A_1^{top} - A_1(x,y))}{A_1^{top}A_1(x,y)}\right)$$

$$\alpha = \ln\left(\frac{A_0^{ho}}{A_0^{top}}\right)\frac{A_1^{top}A_1^{ho}}{A_1^{top} - A_1^{ho}}. \qquad [2]$$

The numerical values used for the constants are $\delta = 17.2$; $A_0^{top} = 1675289$ meV; $A_1^{top} = 0.32324$ Å; $A_2^{top} = 8441$ meV Å^3; $A_0^{ho} = 689527$ meV; $A_1^{ho} = 0.36221$ Å; and, $A_2^{ho} = 8694$ meV Å^3. This potential displays minima in correspondence of Cu atoms (top sites), maxima at the interstitial (hollow) sites and saddles at the bridge sites (20), reproducing the peculiar anticorrugation property observed in these kind of systems (21, 22). We notice here that if the potential would be approximated as a sum of pairwise Lennard-Jones interactions between gas and metal atoms, it would not capture this feature, distorting the estimate of the friction force.

Details of the Molecular Dynamics Simulations. We consider a monolayer of $N = 2048$ Xe atoms interacting with the substrate by the potential discussed above and among themselves via a Lennard-Jones potential

$$W(r) = 4\epsilon\left[\left(\frac{\sigma}{r}\right)^{12} - \left(\frac{\sigma}{r}\right)^6\right], \qquad [3]$$

with $\sigma = 3.98$ Å, $\epsilon = 20$ meV. Equilibrium temperature was controlled by means of a Nosé-Hoover thermostat acting on $3N - 3$ degrees of freedom, i.e. excluding the center of mass motion. The Xe monolayer is equilibrated in its ground state configuration which is a commensurate $(\sqrt{3} \times \sqrt{3})R30°$ structure, as observed experimentally (16). The perfect commensurability is consistent with the fact that a very small lattice mismatch is present between the Xe lattice parameter b and a distance $\sqrt{3}a$, where a is the lattice parameter of the hexagonal Cu surface. In this equilibrium configuration, the Xe atoms occupy one of the three equivalent $(\sqrt{3} \times \sqrt{3})$ sublattices which can be identified on the triangular lattice. This perfect commensurability implies a strong pinning for a defect-free layer. A lateral force $F < F_s$ is applied to all the particles along the x direction which correspond to the minimum energy path for our potential. For our system, F_s is the zero temperature static friction force which can be estimated from our potential as $F_s \simeq 2.4$ meV/Å. We simulate the system at constant force until the Xe monolayer center of mass velocity starts to increase rapidly, signaling the onset of slip. Simulations are repeated several times to obtain reliable statistics. We also use different values of the lateral force and the applied temperature.

Results

The Onset of Frictional Slip. In Fig. 1, we report the time t_0 required to set the system into motion under a constant lateral force F as a function of temperature T. The linearity of semilogarithmic plot of the activation time t_0 as a function of the inverse temperature reveals an Arrhenius law $\log(t_0) = C + U/k_B T$, where U is the activation barrier. The lateral force is varied from $F = 0.55F_s$ to $F = 0.84F_s$ and the energy barrier is found to decrease from $U = 409$ meV to $U = 61$ meV. By comparing these values with those expected for an isolated Xe atom on Cu substrate, which would range from $U_1 = 0.79$ meV to $U_1 = 0.51$ meV, one could infer that the global slip is determined by an effective number of particles, $N_c = U/U_1$, ranging from 120–518. These values are smaller than the total number of particles N which should be involved if the film would slide coherently. This observation clearly indicates that the activation process is a collective effect in which Xe interatomic forces play a major role.

To understand the nature of the activation dynamics, we monitor the film configurations following the particle positions on the potential energy surface. In the initial stage of the simulations, Xe
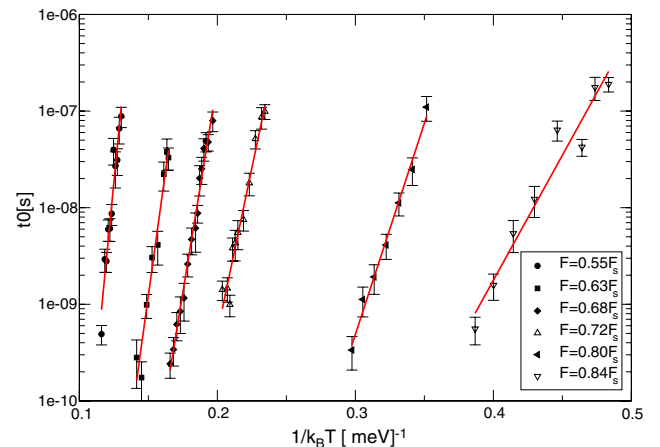

Fig. 1. The activation time as a function of the inverse temperature for different applied lateral forces. The linear behavior in a semilogarithmic plot implies Arrhenius behavior. The slope of the lines yields an estimate of the energy barrier as a function of the applied force.
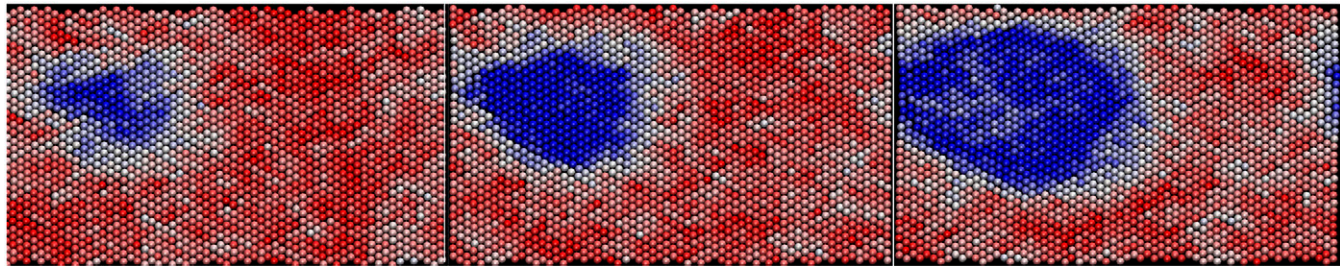
Fig. 2. The formation of a new commensurate domain prior to the global slip. The three images are taken at different times during the slip. The particle color indicates the distance from the substrate potential minima. Red particles are in the original minimum and become blue when they slip into the next minimum. Particles in white are part of the domain wall and are located outside the potential minima.

atoms occupy a set of minima of the substrate potential, until thermal activation leads to the transition to the next set of minima. In Fig. 2 we report a sequence of configurations during this transition. Particles in the original potential minima are colored in red, those in the next minimum in blue and "incommensurate" particles, lying outside of the potential minima, are depicted in white. We observe that the activation process starts with the creation of a small domain of blue particles separated by a domain wall of white particles from the red domain. The blue domain then expands moving the domain wall, until all particles become blue and the system sets into motion under the action of its inertia (a clear idea of this process can be gained observing the supplementary video). The activation process resembles a nucleation process in first order phase transitions, such as the condensation transition or the switching of a ferromagnet in a field. We also notice that domain structures are common in adsorbed layers as intermediate configurations between the commensurate and the incommensurate phases (23, 24).

Theory of Slip Nucleation. The numerical results indicate that the Xe film does not slip coherently from one minimum of the Cu substrate to the next one. A few atoms are displaced in the subsequent minimum forming a new commensurate domain separated by a domain wall from the rest of the film. When the newly nucleated domain is large enough it grows, leading to a global slip of the Xe film by one lattice spacing. The energy change associated with the layer transition from the initial commensurate configuration to the subsequent configuration including a domain of radius r nucleated under a force F can be estimated as

$$\Delta E = 2\pi r \Gamma - \frac{2\pi r^2}{\sqrt{3}b^2} Fa, \qquad [4]$$

where a and b are the lattice spacings of the Cu and Xe films, respectively, and Γ is the energy per unit length of the incommensurate domain wall. The first term in Eq. **4** represents the energy needed to create a domain wall, whereas the second term is the energy gain due to the formation of the new domain. Eq. **4** indicates that for $r < r_c = \frac{\Gamma \sqrt{3}b^2}{2aF}$, domain growth leads to an increase in the energy. Hence, global slip only occurs for $r > r_c$ or when the system overcomes an energy barrier

$$U = \frac{\sqrt{3}\pi \Gamma^2 b^2}{2aF} - E_s, \qquad [5]$$

where we have subtracted the constant $E_s = (\sqrt{3}\pi \Gamma^2 b^2)/(2aF_s)$ because the barrier U should vanish when F reaches the static friction force F_s.

The energy per unit of length Γ associated with a domain wall separating two commensurate domains can be estimated considering a static kink in the Frenkel–Kontorova model (17), in anal-

ogy with the calculation of the energy of Bloch domain walls in ferromagnetic materials (25). It is convenient to define the commensurate domains in terms of the Xe displacement field $u(\mathbf{r}_i) = \mathbf{r}_i - \mathbf{r}_i^0$, where $\mathbf{r}_i^0$ corresponds to the equilibrium position in one of the three equivalent Cu minima. In the continuum limit, the energy of the system can be written as the sum of the elastic energy and the substrate potential (17)

$$E = \int dxdy \left[\frac{1}{2} B(\nabla u)^2 + \rho V(u) \right], \qquad [6]$$

where $\rho = 2/(\sqrt{3}b^2)$ is the density of the Xe film and B is its bulk modulus which can be expressed in terms of the parameters of the interatomic potential as $B \simeq 57\epsilon/\sigma^2$. A domain wall parallel to the y direction is imposed by uniaxial compression of one lattice spacing a. Due to the symmetry of the configuration, the y integral can be eliminated and the problem becomes effectively one dimensional. The substrate potential, when projected along the x direction, is well approximated by

$$V(u) \simeq \frac{V_0}{2}(1 - \cos(2\pi u/a)), \qquad [7]$$

A domain wall of width w emerges from the competition between the elastic energy, roughly scaling as $E_{\mathrm{el}} \simeq Ba^2/w$, and the energy of the substrate potential scaling as $E_{\mathrm{sub}} \simeq V_0 \rho w$. The domain wall width and energy are obtained from the minimization of the sum of these two energies, yielding $w \propto \sqrt{Ba^2/V_0\rho}$ and $\Gamma \propto a\sqrt{\rho BV_0}$. A more precise estimate is obtained performing functional minimization of Eq. **6** and direct integration of the resulting differential equation (17), yielding an implicit solution for the displacement profile

$$x - L/2 = \frac{a\sqrt{2B}}{\pi V_0 \rho} \frac{\log[\tan(\pi u/2a)]\sin(\pi u/a)}{\sqrt{1 - \cos(2\pi u/a)}} \qquad [8]$$

and a quantitative estimate of Γ, including the prefactor,

$$\Gamma = a\sqrt{2\rho BV_0} \int_0^1 dx \sqrt{(1 - \cos(2\pi x))} = \frac{4a}{\pi} \sqrt{2\rho BV_0}. \qquad [9]$$

Inserting the expressions for B and ρ, we obtain $\Gamma \simeq 3.84\sqrt{\epsilon V_0}/a$.

In order to test the theoretical prediction for the displacement profile and the domain wall energy, we induce a static domain wall in the numerical model by using fixed boundary conditions along the x direction. In practice, the rows of atoms at the two edges of the sample are held fixed in one minimum of the substrate potential. An incommensurate domain wall is formed by shifting the first row by a distance a along the positive or negative x direction and equilibrating the system (see Fig. 3). We compute the displacement profile $u(x)$ by averaging the atom positions over the y directions and the domain wall energy as the difference
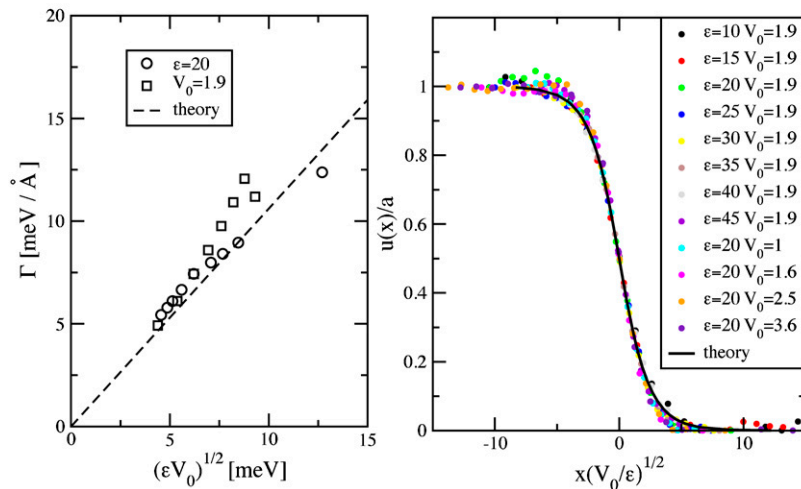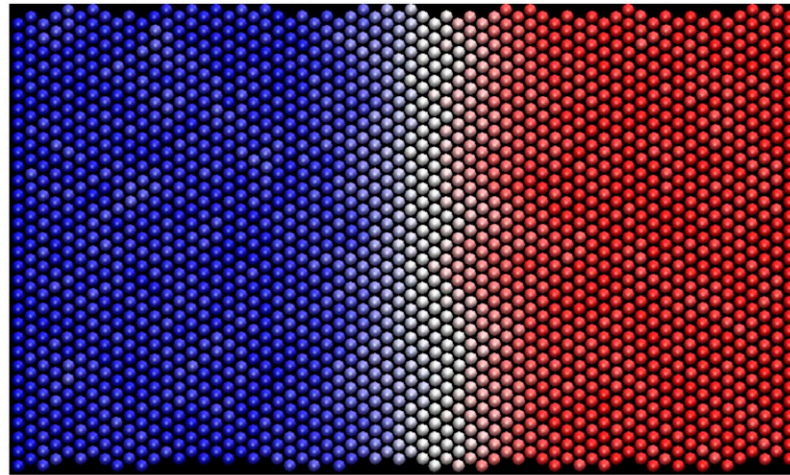
Fig. 3. (*Top*) A typical domain wall obtained in a system with fixed boundaries. (*Bottom left*) The domain wall energy is computed for different values of the interaction strength ϵ and the corrugation of the substrate potential V_0. The domain wall energy scales as a straight line when plotted against $\sqrt{\epsilon V_0}$ in agreement with the continuum theory. (*Bottom right*) The corresponding displacement profiles can all be rescaled into a single curve dividing by the domain wall width $\sqrt{\epsilon/V_0}$ in agreement with the theory.

between the energies of the system with a shifted boundary and the one with unshifted boundaries. The simulation is then repeated for different values of the substrate potential V_0 and the interatomic energy ϵ. The results are shown in Fig. 3 and are in excellent agreement with the theory, considering that no adjustable parameters are involved.

Having established the dependence of the domain wall energy Γ on the relevant atomic interactions, ϵ and V_0, we can now turn back to the nucleation process. Inserting Eq. **9** into Eq. **5**, we predict that $U \propto V_0\epsilon(1/F - 1/F_s)$. In Fig. 4 we plot the activation energy U obtained from the simulations described in Fig. 1, as well as a new set of simulations in which we vary V_0 and ϵ, and find a very good agreement with the theory. In addition, the theoretical value of the critical domain size N_c is given by $N_c = \pi r_c^2\rho$. By considering an external force ranging from $F = 0.55F_s$ to $F = 0.84F_s$, N_c varies from $N_c = 424$ to $N_c = 173$, in agreement with the simulation results. We can thus conclude that creep sliding of a Xe monolayer on a Cu substrate is described by a domain nucleation process.

The Role of Defects. The close relation between the onset of slip and classical nucleation suggests additional considerations. In the model we have concentrated on a perfect system without any defect in the film or in the substrate, a case that corresponds to homogeneous nucleation. In general, impurities should strongly favor the nucleation process, providing seeds for the development

of the new phase, a process commonly referred as heterogeneous nucleation. Defects, such as vacancies or surface steps, are commonly observed in adsorbed monolayers and are expected
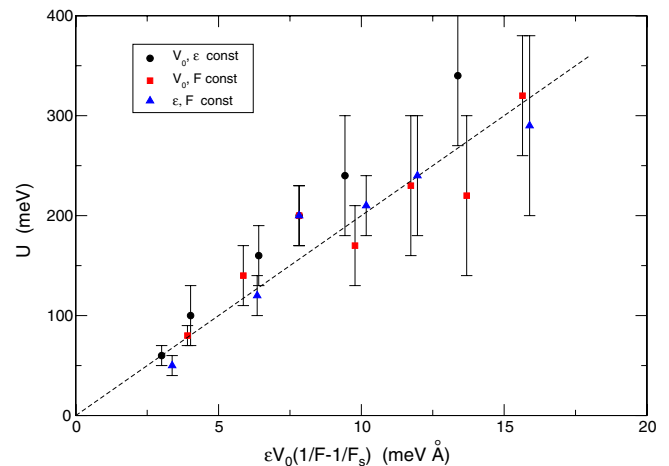

Fig. 4. The activation energies obtained for different values of the interatomic interaction ϵ, the substrate potential V_0 and the lateral force F. In the three datasets, we keep two parameters constant and vary the other one. All the data can all be collapsed into a single line when plotted against $\epsilon V_0(1/F - 1/F_s)$ as predicted by nucleation theory (Eq. **5**).
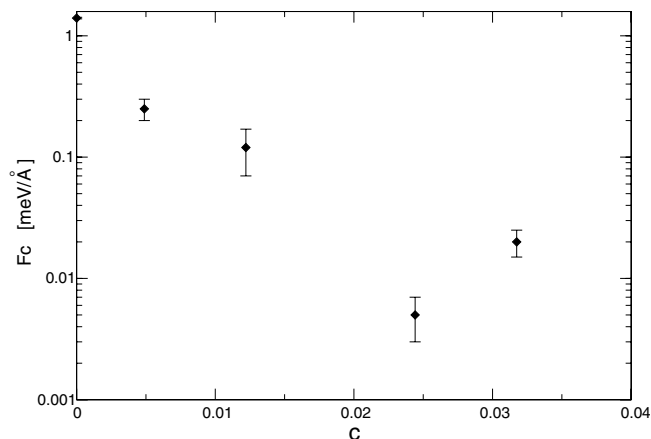
Fig. 5. The effective depinning force F_c as a function of the concentration of vacancies. The depinning force has been obtained as the value of the force for which half of $N_r = 10$ different configurations depin after a time $t_e = 10^{-7}$ s. The error bar is estimated considering the forces for which the fraction of depinned configurations lies between $p = 0.2$ and $p = 0.8$.

to affect the frictional properties, possibly reducing the nucleation barrier. To quantify the role of defects in the nucleation process, we have repeated our simulations introducing a small concentration c of vacancies in the Xe monolayer. To obtain an estimate of the effective depinning force F_c at which the monolayer starts to slide, we analyze the dynamics of the system for a fixed time $t_e = 10^{-7}$ s. We start the system from different equilibrated initial conditions and compute the fraction $p(F)$ of configurations whose center of mass moves by at least one lattice spacing after a time t_e under a lateral force F. The fraction $p(F)$ crosses over from $p = 1$ to $p = 0$ as the force is decreased and we can thus define the depinning force from the condition $p(F_c) = 1/2$. The result reported in Fig. 5 shows a drastic reduction of the depinning force as a function of the concentration of vacancies. For $c = 0.024$, the depinning force is reduced by a factor 10^3 with respect to the value of the pure system. When c is further increased, however, the depinning force appears to grow again. This behavior can be understood considering the particle configurations as a function of the vacancy concentration. As c is decreased, vacancies induce the formation of a small commensurate domain that acts as the seed of the nucleation process. For $c = 0.024$, the structure of the film is reminiscent of the uniaxially incommensurate phase with two striped domains separated by a domain wall parallel to the y direction (23, 24). In this case the film slips forward by displacing the domain wall, without the need to nucleate a new domain. As the vacancy concentration is further increased, the two large domains will eventually split into several commensurate subdomains, increasing the effective depinning force.

Comparison with QCM Experiments. Although usually commensurate interfaces do not slide in the QCM because the applied lateral force is too low to depin the film from the substrate, a recent experiment showed a Xe film would slide on a Cu substrate (11). A typical QCM operates at the resonance frequency of $\omega_0 \simeq 10^7$ s^{-1} with an amplitude $A \simeq 100$ Å, corresponding to a maximum lateral inertial force on the monolayer $F_{QCM} = m\omega_0^2 A \simeq 10^{-7}$ meV/Å. In order for the film to slide, the nucleation time should be smaller than the experimental time scale. This would be clearly impossible for a perfect system: If we extrapolate from Eq. 5, we estimate a barrier $U \simeq 10^7$ eV that

would yield an astronomical activation time. This confirms the well known fact that commensurate interfaces remain pinned in the QCM (12). On the other hand, displacing a preexisting domain wall requires a much lower force than the one needed to nucleate a new commensurate domain. A domain configuration, similar to the one observed in the intermediate stage between the commensurate and the incommensurate phase of triangular layers such as Xe on Pt(111) (26), can be induced in commensurate interfaces for various reasons, such as vacancies in the film as discussed above, or other defects in the substrate, and could provide the key to interpret the QCM experiments reported in ref. (11). Domain walls are pinned by the so called Peierls–Nabarro potential, that can be estimated as (17)

$$V_{PN} \simeq 64\pi^2 g V_0 \exp(-\pi^2 \sqrt{g}), \qquad \text{[10]}$$

where $g = \frac{2a^2 B}{(2\pi)^2 b^2 V_0 \rho}$ is the rescaled coupling constant. Using the parameters for the Xe/Cu interface, we obtain $V_{PN} \simeq 10^{-6}$ meV. Such a low barrier could be easily overcome by thermal activation even under the inertial forces provided by the QCM. This result suggests that the results of ref. (11) are very likely due to the displacement of preexisting domain walls.

Discussion

In this paper, we have studied the onset of slip in a monolayer film of Xe adsorbed on a Cu surface by molecular dynamics simulations. We have considered thermal-activated motion of the Xe monolayer under an applied lateral force, and found that frictional slip occurs by the nucleation of a small commensurate domain that then expands by displacing a domain wall. The process is very similar to the switching of a ferromagnet in a field or the classical bubble nucleation in condensation transitions. Thanks to this analogy, we can use the classical theory of nucleation to interpret the numerical results. The onset of slip can be characterized in terms of the energy changes associated to a new commensurate domain. Domain formation is favored by the applied lateral force and is hindered by the energy cost associated with a domain wall. Hence only when the domain size reaches a critical value, the growth becomes irreversible, setting the monolayer into motion. Nucleation theory allows us to obtain an estimate of the nucleation energy barrier that can then be directly compared with the result of molecular dynamics simulation. A key role in this comparison is played by the domain wall energy which can be estimated in the continuum limit. The result is in excellent quantitative agreement with the simulations. To obtain further confirmation of this result, we vary the strength of the interatomic interaction and the corrugation of the substrate potential. We find that the nucleation energy barrier depends linearly on both quantities, in good agreement with the theoretical prediction. We thus conclude that domain nucleation and domain wall propagation are the dominant mechanisms ruling the slip of commensurate layers. Finally, we have studied the role of disorder in the nucleation process and shown that it strongly reduces the nucleation barrier. This could be the key to understanding experimental results on a Xe/Cu interface displaying sliding despite the commensurate structure. The experiments can be explained if we assume the presence of disorder-induced domain walls in the system.

1. Heslot F, Baumberger T, Perrin B, Caroli B, Caroli C (1994) Creep, stick-slip, and dry-friction dynamics: Experiments and a heuristic model. *Phys Rev E*, 49:4973–4988.
2. Yang Z, Zhang Y, Marder M (2008) Dynamics of static friction between steel and silicon. *Proc. Natl. Acad. Sci. USA*, 105:13264–13268.

3. Rubinstein SM, Cohen G, Fineberg J (2004) Detachment fronts and the onset of dynamic friction. *Nature*, 430:1005–1009.
4. Gerde E, Marder M (2001) Friction and fracture. *Nature*, 413:285–288.

5. Cieplak M, Smith ED, Robbins MO (1994) Molecular origins of friction: The force on adsorbed layers. *Science*, 265:1209–1212.

6. Persson BNJ (1993) Theory and simulation of sliding friction. *Phys Rev Lett*, 71:1212–1215.

7. Braun OM, Paliy MV, Röder J, Bishop AR (2001) Locked-to-running transition in the two-dimensional underdamped driven frenkel-kontorova model. *Phys Rev E*, 63:036129.

8. Braun OM, Dauxois T, Paliy MV, Peyrard M (1997) Nonlinear mobility of the generalized frenkel-kontorova model. *Phys Rev E*, 55:3598–3612.

9. Granato E, Ying SC (2000) Transverse thermal depinning and nonlinear sliding friction of an adsorbed monolayer. *Phys Rev Lett*, 85:5368–5371.

10. Krim J, Solina DH, Chiarello R (1991) Nanotribology of a kr monolayer: A quartz-crystal microbalance study of atomic-scale friction. *Phys Rev Lett*, 66:181–184.

11. Coffey T, Krim J (2005) Impact of substrate corrugation on the sliding friction levels of adsorbed films. *Phys Rev Lett*, 95:076101.

12. Bruschi L, Carlin A, Mistura G (2002) Depinning of atomically thin kr films on gold. *Phys Rev Lett*, 88:046105.

13. He G, Müser MH, Robbins MO (1999) Adsorbed layers and the origin of static friction. *Science*, 284:1650–1652.

14. Sokoloff JB (2002) Possible microscopic explanation of the virtually universal occurrence of static friction. *Phys Rev B*, 65:115415.

15. Righi MC, Ferrario M (2007) Potential energy surface for rare gases adsorbed on cu (111): Parameterization of the gas/metal interaction potential. *J Phys Condens Matter*, 19:305008–305018.

16. Jupille J, Ehrhardt JJ, Fargues D, Cassuto A (1990) Study of xenon layers on a cu(111) surface. *Faraday Discuss Chem Soc*, 89:323–328.

17. Braun OM, Kivshar YS (2004) *The Frenkel-Kontorova Model: Concepts, Methods, and Applications* (Springer-Verlag, Berlin).

18. Zaremba E, Kohn W (1976) Van der Waals interaction between an atom and a solid surface. *Phys Rev B*, 13:2270–2285.

19. Braun J, Fuhrmann D, Šiber A, Gumhalter B, Wöll C (1998) Observation of a zone-center gap in the longitudinal mode of an adsorbate overlayer: Xenon on cu(111). *Phys Rev Lett*, 80:125–128.

20. Righi MC, Ferrario M (2007) Pressure induced friction collapse of rare gas boundary layers sliding over metal surfaces. *Phys Rev Lett*, 99:176101–176105.

21. Diehl RD, et al. (2004) The adsorption sites of rare gases on metallic surfaces: a review. *J Phys Condens Matter*, 16:S2839–S2862.

22. Silva JLFD, Stampfl C, Scheffler M (2003) Adsorption of xe atoms on metal surfaces: New insights from first-principles calculations. *Phys. Rev. Lett.*, 90:066104.

23. Bruch LW, Cole MW, Zaremba E (1997) *Physical Adsorption: Forces and Phenomena* (Clarendon Press, Oxford).

24. Zangwill A (1988) *Physics at Surfaces* (Cambridge Univ Press, Cambridge, New York).

25. Hubert A, Schäfer R (1998) *Magnetic Domains* (Springer, New York).

26. Kern K, David R, Zeppenfeld P, Palmer R, Comsa G (1987) Symmetry breaking commensurate-incommensurate transition of monolayer xe physisorbed on pt(111). *Solid State Comm*, 62:391–394.